Ultrasonics Sonochemistry xxx (2014) xxx–xxx

Contents lists available at ScienceDirect

Ultrasonics Sonochemistry

journal homepage: www.elsevier.com/locate/ultson

Preparation and sonodynamic activities of water-soluble tetra-α-(3-carboxyphenoxyl) zinc(II) phthalocyanine and its bovine serum albumin conjugate

He-Nan Xu [1], Hai-Jun Chen [1], Bi-Yuan Zheng, Yun-Quan Zheng, Mei-Rong Ke, Jian-Dong Huang *

College of Chemistry and Chemical Engineering, Fuzhou University, Fuzhou, China

ARTICLE INFO

Article history:
Received 1 April 2014
Received in revised form 23 May 2014
Accepted 23 May 2014
Available online xxxx

Keywords:
Phthalocyanine
Serum albumin
Ultrasound
Sonodynamic therapy
Sonosensitizer

ABSTRACT

Sonodynamic therapy (SDT) is a new approach for cancer treatment, involving the synergistic effect of ultrasound and certain chemical compounds termed as sonosensitizers. A water-soluble phthalocyanine, namely tetra-α-(3-carboxyphenoxyl) zinc(II) phthalocyanine ($ZnPcC_4$), has been prepared and characterized. The interactions between $ZnPcC_4$ and bovine serum albumin (BSA) were also investigated by absorption and fluorescence spectroscopy. It was found that there were strong interactions between $ZnPcC_4$ and BSA with a binding constant of $6.83 \times 10^7\ M^{-1}$. A non-covalent BSA conjugate of $ZnPcC_4$ ($ZnPcC_4$–BSA) was prepared. Both $ZnPcC_4$ and $ZnPcC_4$–BSA exhibited efficient sonodynamic activities against HepG2 human hepatocarcinoma cells. Compared with $ZnPcC_4$, conjugate $ZnPcC_4$–BSA showed a higher sonodynamic activity with an IC_{50} value of 7.5 μM. Upon illumination with ultrasound, $ZnPcC_4$–BSA can induce an increase of intracellular reactive oxygen species (ROS) level, resulting in cellular apoptosis. The results suggest that the albumin conjugates of zinc(II) phthalocyanines functionalized with carboxyls can serve as promising sonosensitizers for sonodynamic therapy.

1. Introduction

Sonodynamic therapy (SDT) is a new approach for cancer treatment, which was developed on the basis of photodynamic therapy (PDT) [1–3]. PDT utilizes the combined action of photosensitizer, light, and molecular oxygen to eradicate cancer cells [4,5]. However, clinical application of PDT is limited to the treatment of superficial and small solid tumors due to the poor tissue penetration of excitation light [6]. Similarly to PDT, SDT utilizes the combined action of a sonosensitizer and low-intensity ultrasound to cause cell and tissue damage. Ultrasound has an appropriate tissue attenuation that lets it penetrate and reach deep-seated tissues without losing ability to focus energy into small volume. This unique advantage makes SDT more efficient for noninvasive treatment of deep-seated tumors compared with PDT [7–10]. Accumulating evidences indicate that SDT has a great potential in cancer therapy [11–15].

The overall efficacy of sonodynamic therapy depends greatly on the behavior of the sonosensitizer. To date, the most common sonosensitizers are porphyrin derivatives such as hematoporphyrin (the first generation photosensitizer), portoporphyrin IX, and ATX-70 (a gallium porphyrin complex) [7,16]. Nonetheless, these porphyrin-based sonosensitizers have some shortcomings such as skin photosensitivity and unsatisfactory sonocytotoxicity. Significant efforts have therefore been put in new sonosensitizers which have better sonochemical properties, higher tumor specificity, and less skin photosensitivity.

Phthalocyanines have been proposed as highly promising photosensitizers over the last three decades, owing to their intense absorption in the red visible region, high efficiency to generate reactive oxygen species, low dark toxicity, and low skin photosensitivity [17–19]. However, the use of phthalocyanines as sonosensitizers for SDT remains relatively little studied [20–23]. Herein, we reported the preparation and *in vitro* sonodynamic activities of a tetra-α-(3-carboxyphenoxyl) zinc(II) phthalocyanine ($ZnPcC_4$) and its bovine serum albumin conjugate ($ZnPcC_4$–BSA). Zinc(II) phthalocyanines functionalized with carboxyl(s) have been used as efficient photosensitizers, due to their water solubility and high singlet oxygen yield [24–26]. However, the sonodynamic activity of this type of phthalocyanine has not been investigated. In addition, despite recent advances using serum albumin as the protein carrier for anticancer drugs or photosensitizers to improve their

* Corresponding author. Tel.: +86 591 22866235; fax: +86 591 22866227.
E-mail address: jdhuang@fzu.edu.cn (J.-D. Huang).
[1] These authors contributed equally to this work.

http://dx.doi.org/10.1016/j.ultsonch.2014.05.019
1350-4177/

passive targeting properties [27–29], to the best of our knowledge, the application of serum albumin for delivery of sonosensitizer has no precedents in the literature.

2. Experimental

2.1. General

All the reactions were performed under an atmosphere of nitrogen. *N*,*N*-dimethylformamide (DMF) was dried over molecular sieves and further distilled under reduced pressure before use. Potassium carbonate was activated by muffle at 300 °C under normal pressure. Chromatographic purifications were performed on silica gel columns (100–200 mesh, Qingdao Haiyang Chemical Co., Ltd., China) with the indicated eluents. Bovine serum albumin was purchased from Sigma–Aldrich Co. All other solvents and reagents were of reagent grade and used as received.

^{1}H NMR spectra were recorded on a Bruker AVANCEIII 400 spectrometer (400 MHz). Chemical shifts were relative to internal $SiMe_4$ (δ = 0 ppm). Mass spectra were recorded on a Finnigan LCQ Deca xpMAX mass spectrometer. IR spectra were recorded on a Perkin-Elmer SP2000 FT-IR spectrometer, using KBr disks. Elemental analyses were performed by Element Vario EL III equipment. Electronic absorption spectra were measured on a Shimadzu UV-2450 UV–vis spectrophotometer. Fluorescence spectra were taken on an Edinburgh FL900/FS900 spectrofluorometer. The fluorescence quantum yields (Φ_F) were determined by the equation: $\Phi_{F(sample)} = (n^2_{sample}/n^2_{ref})\cdot(F_{sample}/F_{ref})\cdot(A_{ref}/A_{sample})\,\Phi_{F(ref)}$, where *F*, *A*, and *n* are the measured fluorescence (area under the emission peak), the absorbance at the excitation position, and the refractive index of the solvent, respectively. Unsubstituted zinc(II) phthalocyanine (ZnPc) in DMF [$\Phi_{F(ref)}$ = 0.28] was used as the reference [30]. The singlet oxygen quantum yields (Φ_Δ) was measured in DMF by a steady-state method using 1,3-diphenylisobenzofuran (DPBF) as the scavenger and ZnPc [$\Phi_{\Delta(ref)}$ = 0.56] as reference [31,32].

2.2. Synthesis of $ZnPcC_4$

2.2.1. 3-(3-carboxyphenoxyl)phthalonitrile (α-C)

A mixture of 3-nitrophthalonitrile (0.87 g, 5 mmol), 3-hydroxybenzoic acid (0.69 g, 5 mmol), and anhydrous K_2CO_3 (2.07 g, 15 mmol) in dry DMSO (20 mL) was stirred at room temperature for 24 h under nitrogen atmosphere. The reaction mixture was filtered by sand core funnel and the filtrate was poured into ice water (200 mL). Subsequently, HCl aqueous solution (2 M) was added to the filtrate until pH = 1–3 to give white precipitate, which was collected by filtration, washed with water until pH = 7 and dried in vacuum. The crude product was purified by recrystallization with DMF/water to afford white solid (1.11 g, 84%). R_f = 0.53 (EtOH). IR (KBr, cm^{-1}): 3078.4 (Ar–H); 1585.6, 1466.7, 1450.9 (C=C, Ar); 1303.7, 1278.7, 1208.9 (Ar–O–Ar); 2232.9 (C≡N); 1688.8 (C=O). MS (ESI): m/z 263.1 $[M-H]^-$. ^{1}H NMR (DMSO-d_6, ppm): δ 13.16 (br., 1H), 7.81–7.88 (m, 3H), 7.62–7.67 (m, 2H), 7.52 (t, *J* = 0.6 Hz, 1H), 7.32 (d, *J* = 4.2 Hz, 1H). Anal. Calcd for $C_{15}H_8N_2O_3$: C, 68.18; H, 3.05; N, 10.60. Found: C, 67.99; H, 3.27; N, 10.86.

2.2.2. 1,8(11),15(18),22(25)-tetrakis-(3-carboxyphenoxyl) zinc(II) phthalocyanine ($ZnPcC_4$)

A mixture of 3-(3-carboxyphenoxyl)phthalonitrile (0.26 g, 1.0 mmol) and K_2CO_3 (0.14 g, 1.0 mmol) in n-pentanol (20 mL) was stirred at 90 °C under nitrogen atmosphere for 15 min, and then zinc acetate (0.11 g, 0.6 mmol) and 1,8-diazabicyclo[5.4.0]undec-7-ene (DBU) (0.4 mL, 2.6 mmol) were added. The mixture was heated to reflux at 130 °C for 10 h. The solvent was then removed in vacuum and the residue was treated with water and acidified with HCl aqueous solution (1 M) to induce precipitation. The precipitate was collected by filtration, washed with water until pH 7, and dried in vacuum. The crude product was subjected to column chromatography using DMF/ethyl acetate (1:3, v/v) and then DMF as eluents. The last green fraction was collected, and dried in vacuum to give dark green solid (0.10 g, 37%). R_f = 0.67 (MeOH). IR (KBr, cm^{-1}): 3273.8 (O–H); 1702.1 (C=O); 3065.5 (Ar–H), 1577.3, 1481.1, 1440.2 (C=C, Ar); 1247.2 (Ar–O–Ar); 1129.7 (C–N). MS (ESI): m/z 1121.2 $[M+H]^+$. ^{1}H NMR (DMSO-d_6, ppm): δ 9.10–9.28 (m, 2H), 8.68–8.75 (m, 1H), 8.55 (t, *J* = 8.2 Hz, 1H), 8.20 (t, *J* = 7.6 Hz, 1H), 8.07 (t, *J* = 7.6 Hz, 2H), 7.84–7.92 (m, 4H), 7.63–7.73 (m, 17H). Anal. Calcd for $C_{60}H_{32}N_8O_{12}Zn$: C, 64.21; H, 2.87; N, 9.98. Found: C, 64.03; H, 3.01; N, 9.82.

2.3. Preparation of phthalocyanine-BSA conjugate

The non-covalent BSA conjugate of $ZnPcC_4$ was prepared according to the literature procedure [33]. The conjugate was obtained by stirring a mixture of $ZnPcC_4$ and BSA (molar ratio: $ZnPcC_4$/BSA = 2/1) in a phosphate buffered saline (PBS) at ambient temperature overnight, followed by gel chromatography on a G-100 Sephadex column using deionized water as eluent. The conjugate $ZnPcC_4$–BSA collected as the first blue fraction was lyophilized to remove water. The protein content in the conjugate was calculated from the absorbance at 280 nm in a diluted PBS solution (pH = 7.4) with reference to the corresponding molar absorptivity of BSA ($\varepsilon = 4.85 \times 10^4\ M^{-1}\ cm^{-1}$). The phthalocyanine concentration was calculated from the Q band absorbance in a diluted DMF solution with reference to the corresponding molar absorptivity ($\varepsilon = 2.19 \times 10^5\ M^{-1}\ cm^{-1}$).

2.4. In vitro studies

For *in vitro* studies, $ZnPcC_4$ was first dissolved in DMF (1.0 mM) and the solution was diluted to 80 μM with 0.5% (wt.) aqueous solution of Cremophor EL (Sigma, 0.5 g in 100 mL of water). $ZnPcC_4$–BSA conjugate was dissolved in PBS with a concentration of 80 μM. BSA was also dissolved in PBS with a concentration of 80 μM. These solutions were clarified with 0.45 μm filter, and then diluted with the cellular culture medium (as described below) to appropriate concentrations.

Human hepatocellular carcinoma HepG2 cells were obtained from the cell bank of the Chinese Academy of Science, Shanghai, China. The cells were maintained in RPMI 1640 medium (Invitrogen) supplemented with 10% fetal calf serum, streptomycin (50 μg mL^{-1}), and penicillin (50 units mL^{-1}). The cells were incubated at 37 °C in a humidified CO_2 (5%) incubator, and the medium was refreshed every 1–2 days. Cells in the exponential phase of growth were used in the following experiments.

2.4.1. Sonodynamic activity assay

HepG2 cells were exposed to ultrasound after an incubation of 45 min with $ZnPcC_4$–BSA, $ZnPcC_4$, and BSA, respectively. The experimental set-up for ultrasound exposure is showed in Fig. 1. The transducer with a diameter of 45 mm was submerged in the stainless steel container filled with cold degassed water. Polystyrene tube containing 0.5 mL of cell suspension (2×10^5 cells mL^{-1} in RPMI 1640 medium) was fixed vertically on the focal area of the transducer. The distance between the bottom of the polystyrene tube and the transducer was 1 cm. The spatial average ultrasonic intensity was 2.0 W cm^{-2} with a frequency of 1.0 MHz in continuous waves and the ultrasonic time was set at 3 min. The ultrasound system (Therapy Ultrasound 4150) was manufactured by the CARCI Company. For all experiments, the cold degassed water was used as the ultrasonic coupling medium, thereby reducing

Please cite this article in press as: H.-N. Xu et al., Preparation and sonodynamic activities of water-soluble tetra-α-(3-carboxyphenoxyl) zinc(II) phthalocyanine and its bovine serum albumin conjugate, Ultrason. Sonochem. (2014), http://dx.doi.org/10.1016/j.ultsonch.2014.05.019

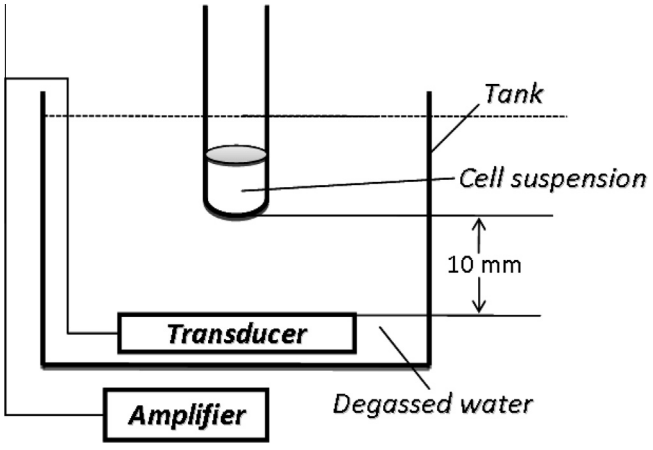

Fig. 1. Diagram of ultrasonic exposure apparatus.

thermal effect caused by ultrasound irradiation. All experiments were randomly divided into eight groups: $ZnPcC_4$–BSA mediated SDT, $ZnPcC_4$ mediated SDT, BSA mediated SDT, ultrasound treatment alone, and the controls including $ZnPcC_4$–BSA, $ZnPcC_4$, and BSA treatment alone and sham group. For the sham group, the cells were not treated neither by ultrasound nor any compound incubation. All the experiments were performed in the dark.

The 3-(4,5-dimthylthiazol-2-yl)-2,5-diphenyl-tetrazolium bromide (MTT) assay was used to determine the cell viability. After SDT treatment, the treated cells or control cells (100 μL) were seeded on a 96-well plate and incubated overnight at 37 °C under 5% CO_2. The medium was then removed from each well. After that, a 10 μL of MTT solution (5 mg mL^{-1} in PBS) and 90 μL of the medium were added into each well, followed by incubation for 4 h at 37 °C under 5% CO_2. Subsequently, the MTT-containing medium was removed and 150 μL DMSO was added into each well. After shaking for 10 min, the optical density (OD) at 490 nm was measured using microplate reader (MULTISKAN MK3, Thermo SCIENTIFIC). The killing rate was calculated using the following equation:

$$\text{Cytotoxicity } (\%) = (\text{OD sham group} - \text{OD treatment group}) / \text{OD sham group} \times 100\%.$$

2.4.2. Apoptosis

After SDT treatment, HepG2 cells were seeded in 6-multiwell plates and incubated for 24 h at 37 °C under 5% CO_2. Apoptosis was then analyzed using a flow cytometer (Coulter EpicsXL Beckman, USA) with Annexin V-FITC (fluorescein isothiocyanate) and propidium iodide (PI) staining. Apoptosis Detection Kit (KeyGEN BioTECH, Nanjing, China) was used in the present study. The treated cells were trypsinized to obtain single cell suspension and washed twice with PBS. The obtained cell pellets were re-suspended in 500 μL of the binding buffer, and then added with a mixture of Annexin V-FITC (5 μL) and PI (5 μL) working solution and then incubated at 37 °C for 15 min. After that, the samples were analyzed using the flow cytometer.

2.4.3. Evaluation of reactive oxygen species

Intracellular reactive oxygen species (ROS) production was assessed with a flow cytometer by measuring the fluorescence intensity of dichlorofluorescein (DCF) as described by other researchers [34]. The probe 2,7-dichlorodihydrofluorescein diacetate (DCFH-DA) was purchased from Sigma and dissolved in DMSO to produce a stock solution (1 mM). DCFH-DA, a non-fluorescent cell-permeant compound, is deacetylated by intracellular esterase and converted to the reduced probe dichlorodihydrofluorescein (DCFH), which can be rapidly oxidized to the highly fluorescent product DCF in the presence of ROS. After SDT treatment, HepG2 cells were incubated with DCFH-DA (10 μM, dilute in serum-free medium) for 2 h at 37 °C under 5% CO_2. The cells were then washed with PBS and analyzed immediately by flow cytometer through FL-1 filter with an excitation wavelength of 488 nm.

2.4.4. Cellular uptake

HepG2 cells (2×10^5) were incubated with a solution of $ZnPcC_4$ or $ZnPcC_4$–BSA in the medium (10 μM, 1 mL) for 0, 15, 30, 45, 60, and 75 min, respectively. In each time point, the cells were collected by centrifugation (3 min, 3000 rpm) and washed with PBS. After removing the PBS, the cells were lyzed with DMF (2 mL). The mixture was sonicated for 10 min and then centrifuged at 15,000 rpm for 5 min. The fluorescence spectrum of the supernatant was recorded in an Edinburgh FL900/FS900 spectrofluorometer (excited at 610 nm and monitored emission at 630–800 nm). From the area of emission peak, the concentration of $ZnPcC_4$ in the solution was determined by comparison with a calibration curve obtained with standard solutions of $ZnPcC_4$. Each experiment was repeated three times.

2.5. Statistics

Data were expressed as mean ± standard deviation (SD). Statistical analyses were performed using Student's *t*-test. *P* values less than 0.05 were considered statistically significant.

3. Results and discussion

3.1. Synthesis and photophysical properties of $ZnPcC_4$

Scheme 1 shows the synthetic route of tetra-α-(3-carboxyphenoxyl) zinc(II) phthalocyanine ($ZnPcC_4$). Firstly, a nucleophilic substitution reaction occurred between 3-nitrophthalonitrile and 3-hydroxybenzoic acid under alkaline condition to give the precursor 3-(3-carboxylphenoxy)phthalonitrile (α-C). The precursor α-C was further underwent a cyclotetramerization in the presence of zinc acetate and K_2CO_3 in n-pentanol using DBU as a catalyst to afford the tetra-substituted phthalocyanine $ZnPcC_4$. As reported previously [25,35], anhydrous K_2CO_3 was added to inhibit the possible esterification between the carboxylic groups and the solvent of n-pentanol. The prepared compounds were characterized by ^1H NMR, MS, elemental analyses, and FT-IR spectroscopic methods.

The photophysical and photochemical properties of $ZnPcC_4$ were measured in DMF. As shown in Fig. 2A, $ZnPcC_4$ gave a typical absorption spectrum of non-aggregated phthalocyanines, exhibiting a sharp and intense Q-band at 688 nm. Upon excitation at 610 nm, it showed a strong fluorescence at 702 nm with a fluorescence quantum yield (Φ_F) of 0.11 relative to unsubstituted zinc(II) phthalocyanine (ZnPc) (Φ_F = 0.28) (Fig. 2B and Table 1). To evaluate the photosensitizing efficiency of $ZnPcC_4$, its singlet oxygen quantum yields (Φ_Δ) was also determined by a steady-state method with 1,3-diphenylisobenzofuran (DPBF) as the scavenger. It was found that $ZnPcC_4$ is an excellent singlet oxygen generator with a Φ_Δ value of 0.53. The spectroscopic behavior of $ZnPcC_4$ was further investigated in aqueous solutions. As shown in Fig. 2A, two weak and broad peaks at 651 nm and 697 nm were observed for $ZnPcC_4$ in PBS solution, meanwhile, its fluorescence intensity was very weak relative to that in DMF (Fig. 2B), indicating that $ZnPcC_4$ is aggregated in PBS [26].

Please cite this article in press as: H.-N. Xu et al., Preparation and sonodynamic activities of water-soluble tetra-α-(3-carboxyphenoxyl) zinc(II) phthalocyanine and its bovine serum albumin conjugate, Ultrason. Sonochem. (2014), http://dx.doi.org/10.1016/j.ultsonch.2014.05.019

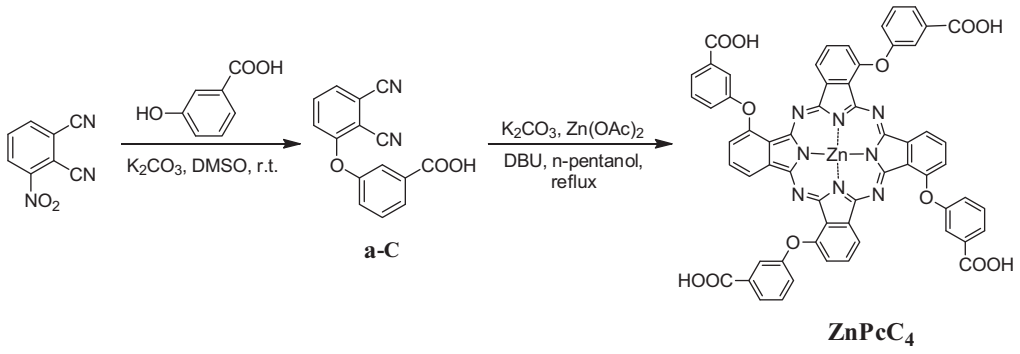

Scheme 1. Synthesis of $ZnPcC_4$.

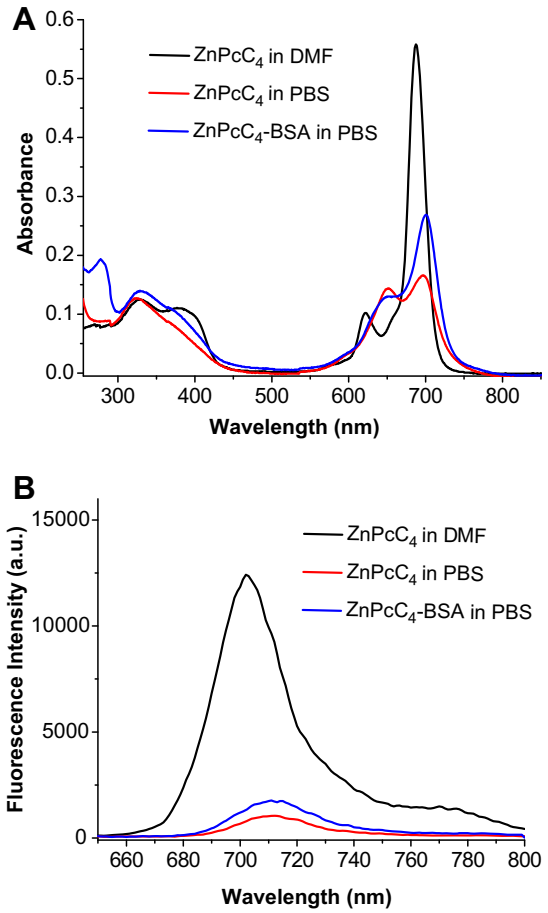

Fig. 2. (A) Electronic absorption and (B) fluorescence emission spectra (excited at 610 nm) of $ZnPcC_4$ and $ZnPcC_4$–BSA (both at 3 μM) in DMF and PBS.

3.2. Interaction and conjugate of $ZnPcC_4$ with BSA

BSA has been used as a carrier for targeted delivery of various anti-cancer drugs [29]. To enhance the biocompatibility and selectivity of phthalocyanine-based sensitizers, attempts were made to prepare the BSA conjugate of $ZnPcC_4$. We firstly analyzed the interactions of $ZnPcC_4$ with BSA by a fluorescence quenching method [36–38]. Fig. 3A shows the change in the fluorescence spectra of BSA in PBS upon titration with $ZnPcC_4$. With the increasing of $ZnPcC_4$, the intrinsic emission band of BSA at 340 nm decreases in intensity. As shown in the inset of Fig. 3A, the quenching data follow the double logarithmic equation (Eq. (1)) [36,39], where F_0 and F are the intensities of fluorescence in the absence and presence of the quencher respectively, C_Q is the concentration of the quencher, K_A is the binding constant, and n is the binding site number. The binding constant K_A and binding site number were found to be $6.83 \times 10^7\ M^{-1}$ and 1, respectively:

$$\lg \frac{F_0 - F}{F} = \lg K_A + n \lg C_Q \quad (1)$$

Table 1
Photophysical data of $ZnPcC_4$ and $ZnPcC_4$–BSA.

Compounds	Solvents	λ_{abs} (nm)	λ_{em}[a] (nm)	$\varepsilon \times 10^5$ ($M^{-1}\cdot cm^{-1}$)	Φ_F[b]	Φ_Δ[c]
$ZnPcC_4$	DMF	688	702	2.19	0.11	0.53
	PBS	651, 697	711	–	0.01	–
$ZnPcC_4$–BSA	PBS	651, 701	711	–	0.02	–

[a] Excited at 610 nm.
[b] Using ZnPc in DMF as the reference ($\Phi_F = 0.28$) [30].
[c] Determined by using DPBF as chemical quencher, and using ZnPc in DMF as the reference ($\Phi_\Delta = 0.56$) [31,32].

On the other hand, upon addition of BSA, the absorption peak at 652 nm of $ZnPcC_4$ in PBS reduced in intensity gradually, while the Q band at 696 nm correspondingly increased in intensity (Fig. 3B). Both this observation and the high K_A indicated that there was a strong interaction between $ZnPcC_4$ and BSA. Furthermore, the Job's plot with titrations (λ_{abs} = 699 nm) at the different concentrations of BSA exhibited a maximum at about 0.5 mol fraction (see the inset in Fig. 3B). This indicates that $ZnPcC_4$ conjugated to BSA with a 1:1 stoichiometry.

In view of the strong interaction between $ZnPcC_4$ and BSA, attempts were made to prepare their non-covalent conjugate according to the literature procedure [33]. The conjugate was obtained by stirring a mixture of $ZnPcC_4$ and BSA (with a molar ratio of 2) in PBS at ambient temperature overnight, followed by a gel chromatography separation step. The molar ratio of phthalocyanine to BSA was found to be 1:1 for the obtained $ZnPcC_4$–BSA conjugate, which is in accord with the result from the Job's plot.

The non-covalent conjugate $ZnPcC_4$–BSA was readily soluble in water. Therefore, its spectroscopic properties were measured in PBS. As shown in Fig. 2A, the Q-band of $ZnPcC_4$–BSA conjugate showed an obvious increase in intensity at 699 nm with slight red-shift compared to that of $ZnPcC_4$. Accordingly, the fluorescence intensity of $ZnPcC_4$–BSA conjugate at 711 nm in PBS was higher than that of $ZnPcC_4$ (Fig. 2B). Moreover, it is need to mention that the spectrum of $ZnPcC_4$–BSA remained virtually unchanged upon standing for long time. These findings strongly suggest that $ZnPcC_4$ is relatively non-aggregated in the protein cavity and $ZnPcC_4$–BSA conjugate is stable in PBS solution.

Please cite this article in press as: H.-N. Xu et al., Preparation and sonodynamic activities of water-soluble tetra-α-(3-carboxyphenoxyl) zinc(II) phthalocyanine and its bovine serum albumin conjugate, Ultrason. Sonochem. (2014), http://dx.doi.org/10.1016/j.ultsonch.2014.05.019

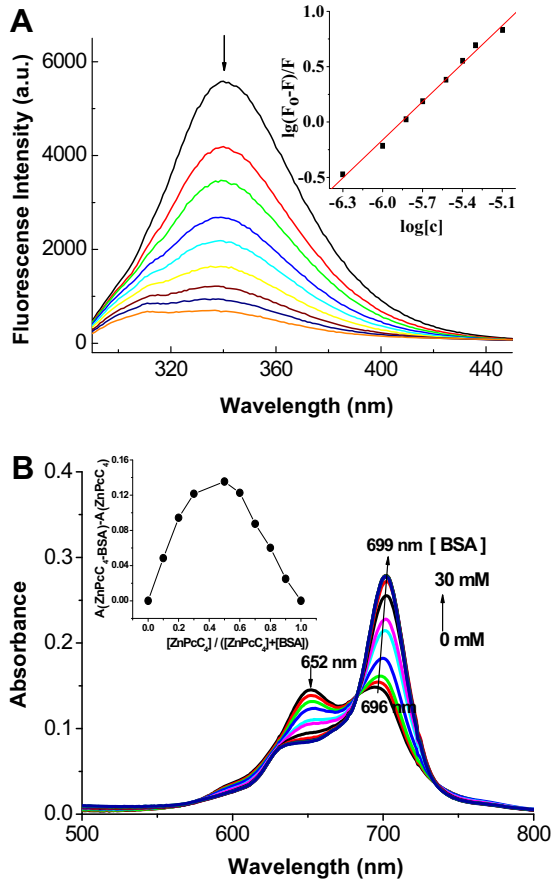

Fig. 3. (A) Change in fluorescence spectrum of BSA (2 μM, excited at 280 nm) in PBS upon titration with $ZnPcC_4$. The inset shows the corresponding $\lg[(F_0 - F)/F]$ vs. $\lg[ZnPcC_4]$ plot. (B) Changes in the absorption spectrum of $ZnPcC_4$ (2 μM) in PBS upon titration with BSA. The inset shows the Job's plot for the binding of ZnPcC4 and BSA (λ_{abs} = 699 nm).

3.3. In vitro sonodynamic anticancer activities

The effects of $ZnPcC_4$, BSA, and $ZnPcC_4$–BSA against HepG2 cells were examined in the absence and presence of ultrasound. In the absence of ultrasound, $ZnPcC_4$, $ZnPcC_4$–BSA, and BSA (all at 10 μM) did not exhibited apparent cytotoxicity on HepG2 cells, as shown in Fig. 4A. When ultrasound treatment alone was used, the cell viability was found to be 86.6%. This suggests ultrasound treatment alone caused slight cellular damage. In the presence of ultrasound, the cell viability caused by BSA was found to be 82.3%, which is comparable with that induced by ultrasound treatment alone (82.3% vs. 86.6%, $p > 0.05$). This indicates that BSA hardly presents sonodynamic activity against HepG2 cells. When HepG2 cells were treated with $ZnPcC_4$ (10 μM) and $ZnPcC_4$–BSA (10 μM) in the presence of ultrasound, the cell viability decreased to 52.0% and 22.9%, respectively. Clearly, both $ZnPcC_4$ and $ZnPcC_4$–BSA exhibited significant sonocytotoxicities toward HepG2 cells ($p < 0.05$ vs. $ZnPcC_4$ alone, $ZnPcC_4$–BSA alone, or ultrasound treatment alone). By comparison, $ZnPcC_4$–BSA showed a higher sonodynamic activity than $ZnPcC_4$ ($p < 0.05$). Further, the concentration-dependent sonocytotoxicity of $ZnPcC_4$–BSA toward HepG2 cells was determined after 45 min of incubation and subsequent illumination with ultrasound. From the dose response curve (Fig. 4B), the IC_{50} value, defined as the sonosensitizer concentration required to kill 50% of cells, was calculated to be 7.5 μM for $ZnPcC_4$–BSA. These results indicate that the photosensitizer $ZnPcC_4$ and its BSA conjugate can serve as efficient sonosensitizers for SDT.

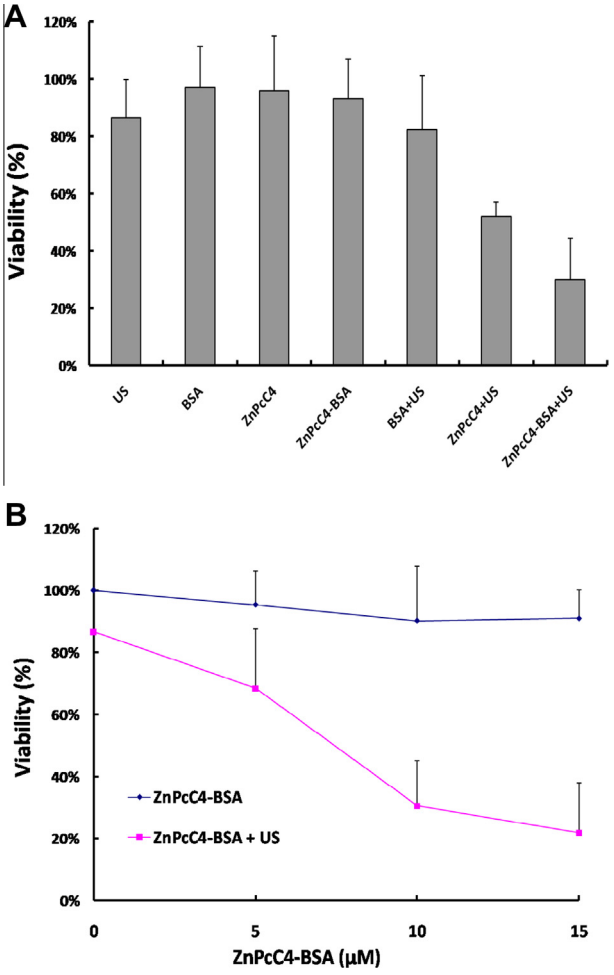

Fig. 4. Effects of $ZnPcC_4$, $ZnPcC_4$–BSA, and BSA on HepG2 cells in the absence and presence of ultrasound (1 MHz, 2.0 W cm^{-2}, 3 min). Data are expressed as mean ± SD ($n \geqslant 6$). (A) The cells were incubated with $ZnPcC_4$, $ZnPcC_4$–BSA, and BSA at the concentration of 10 μM for 45 min before ultrasound illumination. (B) The cells were incubated with $ZnPcC_4$–BSA at the concentration of 0, 5, 10, and 15 μM for 45 min before ultrasound illumination ($p < 0.05$ vs. untreated control).

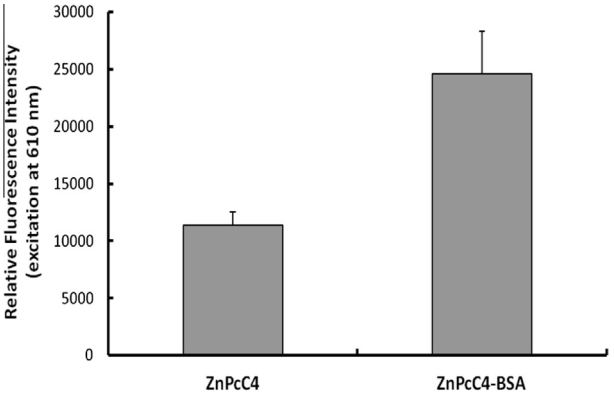

Fig. 5. Cellular uptakes of $ZnPcC_4$ (10 μM) and $ZnPcC_4$–BSA (10 μM) by HepG2 cells after 45 min of incubation.

To account for the different sonodynamic activities of $ZnPcC_4$ and $ZnPcC_4$–BSA, their cellular uptakes were compared by an extraction method. In this method, DMF was used to lyze the cells and extract the photosensitizer. Since the phthalocyanine can be released from BSA cage in DMF, the relative fluorescence intensity of extraction solution can reflect the difference of cellular uptake

Please cite this article in press as: H.-N. Xu et al., Preparation and sonodynamic activities of water-soluble tetra-α-(3-carboxyphenoxyl) zinc(II) phthalocyanine and its bovine serum albumin conjugate, Ultrason. Sonochem. (2014), http://dx.doi.org/10.1016/j.ultsonch.2014.05.019

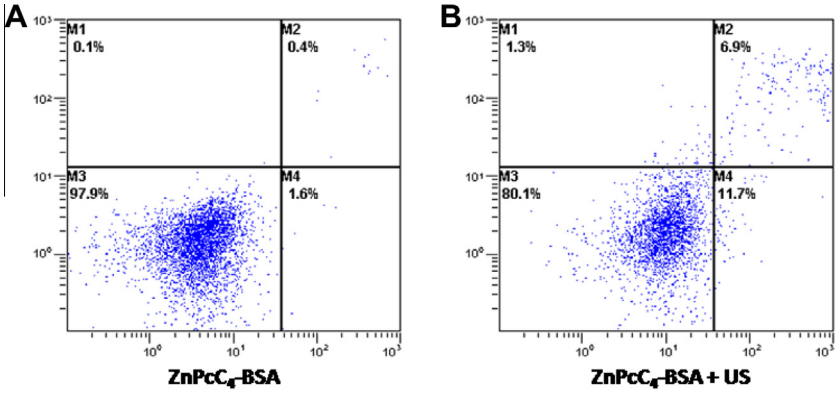

Fig. 6. Flow cytometric analysis of the cell death mechanism induced by SDT treatment (1.0 MHz, 2.0 W cm^{-2}, 3 min) on HepG2 cells with Annexin V-FITC and PI staining. Fluorescence intensity for Annexin V-FITC is plotted on the *X*-axis, and fluorescence intensity for PI is plotted on the *Y*-axis. The bottom right quadrant of each panel shows the early apoptotic cells (Annexin V-FITC positive, PI negative), while the top right quadrant of each panel shows the late apoptotic or necrotic cells (Annexin V-FITC positive, PI positive). (A) Control group ($ZnPcC_4$–BSA alone) and (B) $ZnPcC_4$–BSA-mediated SDT.

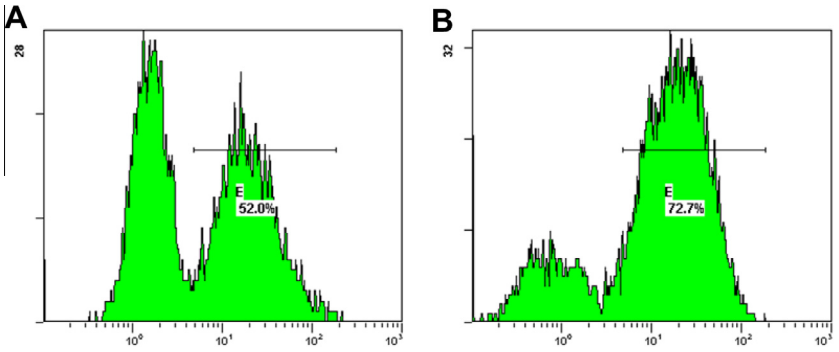

Fig. 7. Flow cytometric analysis of intracellular ROS induced by SDT treatment (1.0 MHz, 2.0 W cm^{-2}, 3 min) on HepG2 cells with DCFH-DA staining. Fluorescence intensity of DCF is plotted on the *X*-axis, and the number of the cells is plotted on the *Y*-axis. (A) Control group (ultrasound alone) and (B) $ZnPcC_4$–BSA-mediated SDT.

between $ZnPcC_4$ and $ZnPcC_4$–BSA. Cellular uptake of $ZnPcC_4$ and $ZnPcC_4$–BSA by HepG2 cells were rapid, which occurred after incubation for 15 min and reached a plateau at 45 min. No further significant uptake was observed over the subsequent 75 min. As shown Fig. 5, after 45 min of incubation, $ZnPcC_4$–BSA conjugate showed about 1.6-fold higher cellular uptake toward HepG2 cells than the free $ZnPcC_4$, which probably results from the high affinity of cancer cells for albumin [28]. Therefore, the higher sonocytotoxicity of $ZnPcC_4$–BSA compared with $ZnPcC_4$ can be mainly attributed to its higher cellular uptake.

3.4. Apoptosis and intracellular reactive oxygen species (ROS)

In order to determinate the possible mechanism of sonodynamic effects caused by $ZnPcC_4$–BSA (10 μM), the flow cytometry with Annexin V-FITC and PI staining was used to distinguish early apoptosis from late apoptosis or necrosis [40]. As shown in Fig. 6, the percentage of cells at early apoptotic stage for $ZnPcC_4$–BSA treatment alone was 1.6%. However, the early apoptotic cell populations for $ZnPcC_4$–BSA-mediated SDT increased to 11.7%. These results show that $ZnPcC_4$–BSA-mediated SDT could induce apoptosis in HepG2 cells. Nevertheless, the number of cells for $ZnPcC_4$–BSA-mediated SDT treatment reduced, suggesting that cell death is not only the result of apoptosis.

Many current studies showed that the cellular toxicity of sonosensitizer could be attributed to the generation of intracellular ROS after exposure to ultrasound [7]. We also attempted to examine whether the intracellular ROS was involved in the process of $ZnPcC_4$–BSA (10 μM)-mediated SDT. The intracellular ROS was evaluated using flow cytometry with DCFH-DA as a ROS probe. As shown in Fig. 7, the fluorescence curves for cells treated by ZnPcC4–BSA-mediated SDT shift to the right compared with that for cells of control group. This indicates that $ZnPcC_4$–BSA caused an obvious increase of ROS generation in the presence of ultrasound. Therefore, it can be reasoned that $ZnPcC_4$–BSA, upon excited by ultrasound, can induce the generation of intracellular ROS, which next leads to the apoptosis or/and necrosis of cancer cells. However, the sonochemical mechanisms of ROS formation induced by $ZnPcC_4$–BSA need further investigation.

4. Conclusions

A new zinc(II) phthalocyanine tetra-substituted with carboxyl groups at α-positions and its BSA conjugate were prepared and characterized. The compound $ZnPcC_4$ is an excellent singlet oxygen generator with a Φ_Δ value of 0.53. Both $ZnPcC_4$ and $ZnPcC_4$–BSA exhibit efficient sonocytotoxicities against HepG2 human hepatocarcinoma cells in the presence of ultrasound. By comparison, $ZnPcC_4$–BSA shows a higher sonodynamic activity with an IC_{50} value of 7.5 μM. To our knowledge, this is the first report about serum albumin conjugates of phthalocyanine as novel sonosensitizers. Further development of such serum albumin conjugates with suitable phthalocyanine may lead us to find a promising sonosensitizer for sonodynamic therapy of cancer.

Acknowledgments

This work was supported by the Natural Science Foundation of China (Grant Nos. 20872016, 21172037), the Natural Science Foundation of Fujian, China (Grant No. 2011J01040), and Specialized

Research Fund for the Doctoral Program of Higher Education (Grant No. 20113514110001).

References

[1] H. Kolarova, K. Tomankova, R. Bajgar, P. Kolar, R. Kubinek, Ultrasound Med. Biol. 35 (2009) 1397.
[2] N. Yumita, R. Nishigaki, K. Umemura, S. Umemura, Jpn. J. Cancer Res. 80 (1989) 219.
[3] S. Umemura, N. Yumita, R. Nishigaki, K. Umemura, Jpn. J. Cancer Res. 81 (1990) 962.
[4] D.E. Dolmans, D. Fukumura, R.K. Jain, Nat. Rev. Cancer 3 (2003) 380.
[5] Z. Huang, Technol. Cancer Res. Treat. 4 (2005) 283.
[6] S.G. Rockson, D.P. Lorenz, W.F. Cheong, K.W. Woodburn, Circulation 102 (2000) 591.
[7] I. Rosenthal, J.Z. Sostaric, P. Riesz, Ultrason. Sonochem. 11 (2004) 349.
[8] K. Tachibana, L.B. Feril Jr., Y. Ikeda-Dantsuji, Ultrasonics 48 (2008) 253.
[9] H. Shibaguchi, H. Tsuru, M. Kuroki, M. Kuroki, Anticancer Res. 31 (2011) 2425.
[10] A.H. Barati, M. Mokhtari-Dizaji, H. Mozdarani, S.Z. Bathaie, Z.M. Hassan, Ultrasound Med. Biol. 35 (2009) 756.
[11] N. Yumita, Y. Iwase, T. Imaizumi, A. Sakurazawa, Y. Kaya, K. Nishi, T. Ikeda, S. Umemura, F.S. Chen, Y. Momose, Anticancer Res. 33 (2013) 3145.
[12] S. Guo, X. Sun, J. Cheng, H. Xu, J. Dan, J. Shen, Q. Zhou, Y. Zhang, L. Meng, W. Cao, Y. Tian, Int. J. Nanomed. 8 (2013) 2239.
[13] H. Tsuru, H. Shibaguchi, M. Kuroki, Y. Yamashita, M. Kuroki, Free Radical Biol. Med. 53 (2012) 464.
[14] Z.J. Dai, S. Li, J. Gao, X.N. Xu, W.F. Lu, S. Lin, X.J. Wang, Med. Hypotheses 80 (2013) 300.
[15] X. Wang, W. Zhang, Z. Xu, Y. Luo, D. Mitchell, R.W. Moss, Integr. Cancer Ther. 8 (2009) 283.
[16] N. Yumita, S. Umemura, R. Nishigaki, In Vivo 14 (2000) 425.
[17] J.P. Celli, B.Q. Spring, I. Rizvi, C.L. Evans, K.S. Samkoe, S. Verma, B.W. Pogue, T. Hasan, Chem. Rev. 110 (2010) 2795.
[18] J.F. Lovell, T.W. Liu, J. Chen, G. Zheng, Chem. Rev. 110 (2010) 2839.
[19] W.M. Sharman, C.M. Allen, J.E. van Lier, Drug Discov. Today 4 (1999) 507.
[20] N. Yumita, S. Umemura, J. Pharm. Pharmacol. 56 (2004) 85.
[21] K. Milowska, T. Gabryelak, Ultrasound Med. Biol. 31 (2005) 1707.
[22] K. Tomankova, H. Kolarova, P. Kolar, K. Kejlova, D. Jirova, Toxicol. In Vitro 23 (2009) 1465.
[23] H. Chen, X. Zhou, Y. Gao, B. Zheng, F. Tang, J.D. Huang, Drug Discov. Today 19 (2014) 502.
[24] C.F. Choi, P.T. Tsang, J.D. Huang, E.Y. Chan, W.H. Ko, W.P. Fong, D.K. Ng, Chem. Commun. (Camb.) (2004) 2236.
[25] M.-R. Ke, J.-D. Huang, S.-M. Weng, J. Photochem. Photobiol. A 201 (2009) 23.
[26] W. Liu, T.J. Jensen, F.R. Fronczek, R.P. Hammer, K.M. Smith, M.G. Vicente, J. Med. Chem. 48 (2005) 1033.
[27] C. Larroque, A. Pelegrin, J.E. Van Lier, Br. J. Cancer 1996 (1886) 74.
[28] W.M. Sharman, J.E. van Lier, C.M. Allen, Adv. Drug Deliv. Rev. 56 (2004) 53.
[29] X.L. Han, F.F. Tian, Y.S. Ge, F.L. Jiang, L. Lai, D.W. Li, Q.L. Yu, J. Wang, C. Lin, Y. Liu, J. Photochem. Photobiol. B 109 (2012) 1.
[30] I. Scalise, E.N. Durantini, Bioorg. Med. Chem. 13 (2005) 3037.
[31] W. Spiller, H. Kliesch, D. Wöhrle, S. Hackbarth, B. Röder, G.J. Schnurpfeil, Porphyrins Phthalocyanines 2 (1998) 145.
[32] M.D. Maree, N. Kuznetsova, T.J. Nyokong, J. Photochem. Photobiol. A 140 (2001) 117.
[33] J.D. Huang, P.C. Lo, Y.M. Chen, J.C. Lai, W.P. Fong, D.K. Ng, J. Inorg. Biochem. 100 (2006) 946.
[34] J. Duranteau, N.S. Chandel, A. Kulisz, Z. Shao, P.T. Schumacker, J. Biol. Chem. 273 (1998) 11619.
[35] Y. Li, T.M. Pritchett, J. Huang, M. Ke, P. Shao, W. Sun, J. Phys. Chem. A 112 (2008) 7200.
[36] Y. Liu, M.X. Xie, M. Jiang, Y.D. Wang, Spectrochim. Acta A 61 (2005) 2245.
[37] E. Alarcon, A.M. Edwards, A.M. Garcia, M. Munoz, A. Aspee, C.D. Borsarelli, E.A. Lissi, Photochem. Photobiol. Sci. 8 (2009) 255.
[38] A. Ogunsipe, T. Nyokong, Photochem. Photobiol. Sci. 4 (2005) 510.
[39] R.P. Xiao, N. Zhang, J.D. Huang, H.H. Zhang, Guang Pu Xue Yu Guang Pu Fen Xi 31 (2011) 1052.
[40] E. Jaruga, S. Salvioli, J. Dobrucki, S. Chrul, J. Bandorowicz-Pikula, E. Sikora, C. Franceschi, A. Cossarizza, G. Bartosz, FEBS Lett. 433 (1998) 287.

Please cite this article in press as: H.-N. Xu et al., Preparation and sonodynamic activities of water-soluble tetra-α-(3-carboxyphenoxyl) zinc(II) phthalocyanine and its bovine serum albumin conjugate, Ultrason. Sonochem. (2014), http://dx.doi.org/10.1016/j.ultsonch.2014.05.019